Phase Segregation in Cs-, Rb- and K-doped Mixed-Cation $(MA)_x(FA)_{1-x}PbI_3$ Hybrid Perovskites from Solid-State NMR

Dominik J. Kubicki,[a] Daniel Prochowicz,[b,c] Albert Hofstetter,[a] Shaik M. Zakeeruddin,[b] Michael Grätzel,*[b] Lyndon Emsley*[a]

[a]*Laboratory of Magnetic Resonance, Institute of Chemical Sciences and Engineering, Ecole Polytechnique Fédérale de Lausanne (EPFL), CH-1015 Lausanne, Switzerland*
[b]*Laboratory of Photonics and Interfaces, Institute of Chemical Sciences and Engineering, Ecole Polytechnique Fédérale de Lausanne (EPFL), CH-1015 Lausanne, Switzerland*
[c]*Institute of Physical Chemistry, Polish Academy of Sciences, Kasprzaka 44/52, 01-224 Warsaw, Poland.*

Table of Contents

Perovskite synthesis

Perovskite powders were synthesized by grinding the substrates in an electric ball mill (Retsch Ball Mill MM-200, a grinding jar (10 ml) and a ball with ⌀10 mm) for 30 min at 30 Hz. Substrates were packed into the jar inside a glove box under argon. The resulting perovskite powders were annealed at 140 °C for 10 minutes to reproduce the thin-film synthetic procedure.[1]

Mixed-cation lead iodide perovskites

FA/Cs perovskite

0.154 g of FAI (0.90 mmol), 0.026 g of CsI (0.10 mmol) and 0.461 g of PbI_2 (1.00 mmol) were mixed to prepare the $(FA)_{0.90}(Cs)_{0.10}PbI_3$ black powder.

0.137 g of FAI (0.80 mmol), 0.052 g of CsI (0.20 mmol) and 0.461 g of PbI_2 (1.00 mmol) were mixed to prepare the $(FA)_{0.80}(Cs)_{0.20}PbI_3$ black powder.

0.120 g of FAI (0.70 mmol), 0.078 g of CsI (0.30 mmol) and 0.461 g of PbI_2 (1.00 mmol) were mixed to prepare the $(FA)_{0.70}(Cs)_{0.30}PbI_3$ black powder.

FA/Rb perovskite

0.154 g of FAI (0.90 mmol), 0.021 g of RbI (0.30 mmol) and 0.461 g (1.00 mmol) of PbI_2 were mixed to prepare the $(FA)_{0.90}(Rb)_{0.10}PbI_3$ black powder.

RbMAFA(I) perovskite

0.039 g of MAI (0.25 mmol), 0.120 g of FAI (0.70 mmol), 0.010 g of RbI (0.05 mmol) and 0.461 g of PbI_2 (1 mmol) were mixed to prepare the $(Rb)_{0.05}(MA)_{0.25}(FA)_{0.70}PbI_3$ black powder.

RbCsFA(I) perovskite

0.146 g of FAI (0.85 mmol), 0.010 g of RbI (0.05 mmol), 0.026 g of CsI (0.10 mmol) and 0.461 g of PbI_2 (1 mmol) were mixed to prepare the $(Rb)_{0.05}(Cs)_{0.10}(FA)_{0.85}PbI_3$ black powder.

RbCsMAFA(I) perovskite

0.039 g of MAI (0.25 mmol), 0.103 g of FAI (0.60 mmol), 0.010 g of RbI (0.05 mmol), 0.026 g of CsI (0.10 mmol) and 0.461 g of PbI_2 (1 mmol) were mixed to prepare the $(Rb)_{0.05}(Cs)_{0.10}(MA)_{0.25}(FA)_{0.60}PbI_3$ black powder.

$K_{0.10}MA_{0.90}PbI_3$ perovskite

0.016 g of KI (0.10 mmol), 0.143 g of MA (0.90 mmol) and 0.461 g (1.00 mmol) of PbI_2 were mixed to prepare the $(K)_{0.10}(MA)_{0.90}PbI_3$ black powder.

Mixed-cation and mixed-halide lead perovskites

MAFA(Br,I) perovskite

The double cation mixed-halide perovskite was fabricated according to the previously published procedure.[1] 0.172 g of FAI (1 mmol), 0.507 g of PbI_2 (1.1 mmol), 0.022 g of MABr (0.2 mmol) and 0.073 g of $PbBr_2$ (0.2 mmol) were milled to prepare the MAFA_(Br,I) black powder.

CsMAFA(Br,I) perovskite

The triple cation perovskite was fabricated according to the previously published recipe.[2] 0.172 g of FAI (1 mmol), 0.507 g of PbI_2 (1.1 mmol), 0.022 g of MABr (0.2 mmol), 0.080 g of $PbBr_2$ (0.22 mmol) and 0.014 g of CsI (0.055 mmol) were milled to prepare the CsMAFA black powder.

RbCsMAFA(Br,I) perovskite

The quadruple cation perovskite was fabricated according to the previously published recipe.[3] 0.172 g of FAI (1 mmol), 0.507 g of PbI_2 (1.1 mmol), 0.022 g of MABr (0.2 mmol), 0.080 g of $PbBr_2$ (0.22 mmol), 0.014 g of CsI (0.055 mmol) and 0.011 g of RbI (0.055 mmol) were milled to prepare the RbCsMAFA black powder.

Rubidium lead bromides

$RbPb_2Br_5$

0.082 g of RbBr (0.5 mmol) and 0.367 g of $PbBr_2$ (1 mmol) were mixed and annealed at 150°C for 15 min to prepare the $RbPb_2Br_5$ white powder.

Rb_4PbBr_6

0.165 g of RbBr (1 mmol) and 0.091 g of $PbBr_2$ (0.25 mmol) were mixed and annealed at 150°C for 15 min.

$Cs_{0.50}Rb_{0.50}PbI_3$

0.128 g of CsI (0.50 mmol), 0.106 g of RbI (0.50 mmol) and 0.461 g of PbI2 (1 mmol) were mixed to prepare the $Cs_{0.50}Rb_{0.50}$PbI3 alloy.

Powder X-ray Diffraction

Diffractograms were recorded on an X'Pert MPD PRO (Panalytical) diffractometer equipped with a ceramic tube (Cu anode, λ = 1.54060 Å), a secondary graphite (002) monochromator and an RTMS X'Celerator (Panalytical) in an angle range of 2θ = 5° to 40°, by step scanning with a step of 0.02 degree.

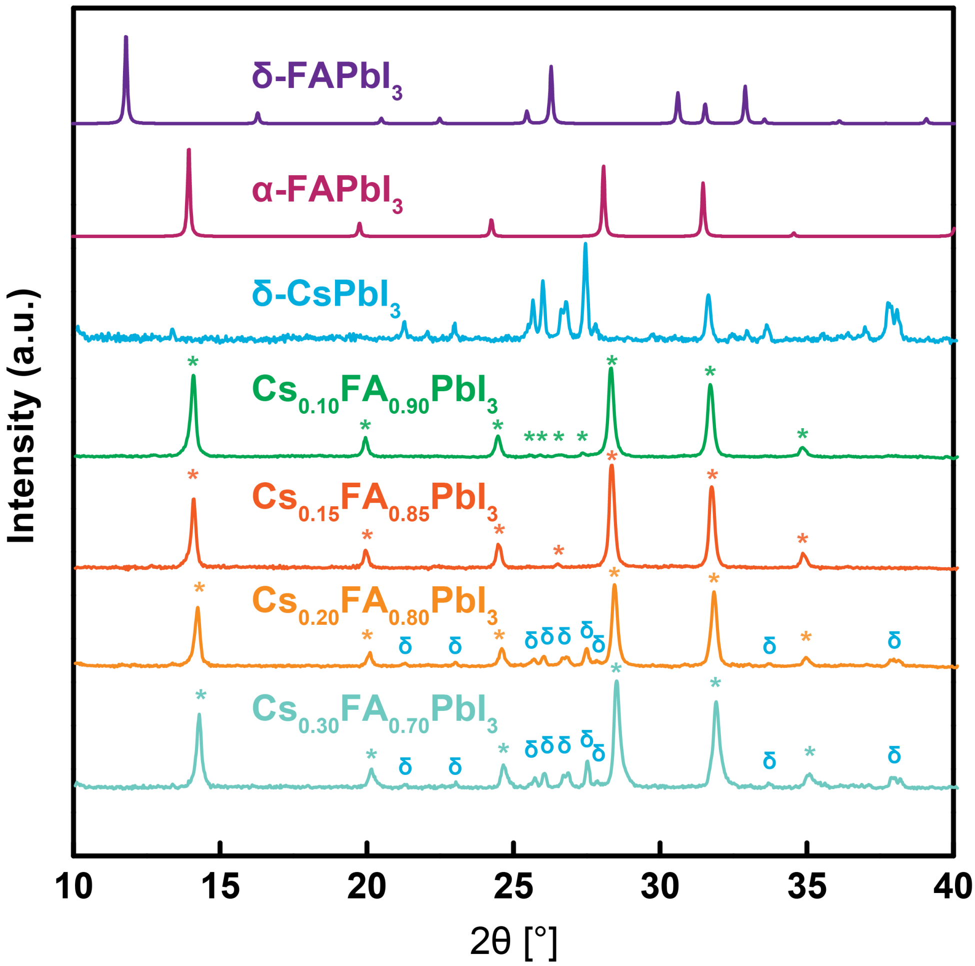

Figure S1. pXRD pattern for the Cs_xFA_{1-x} compositions. Asterisks (*) indicate the primary phases. Deltas (δ) indicate the phase separated δ-CsPbI3.

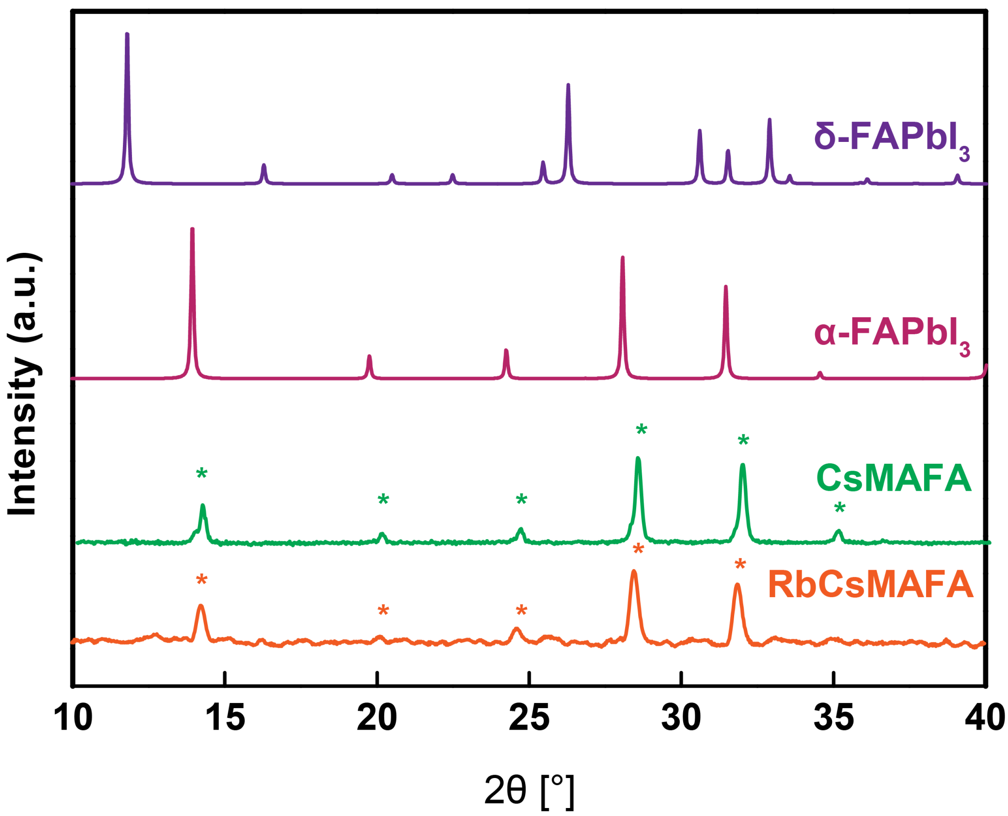

Figure S2. pXRD pattern for the CsFAMA(Br,I) and RbCsMAFA(Br,I) compositions.

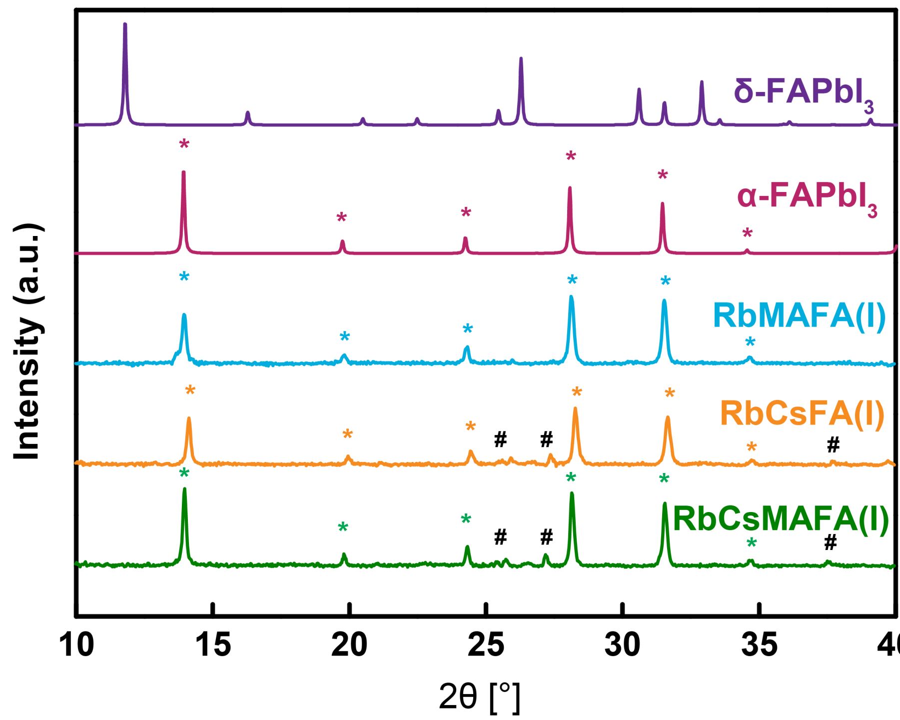

Figure S3. pXRD pattern for the RbMAFA(I), RbCsFA(I) and RbCsMAFA(I) compositions. Asterisks (*) indicate the primary phases. Hashes (#) indicate the mixed $Cs_{0.5}Rb_{0.5}PbI_3$ phase.

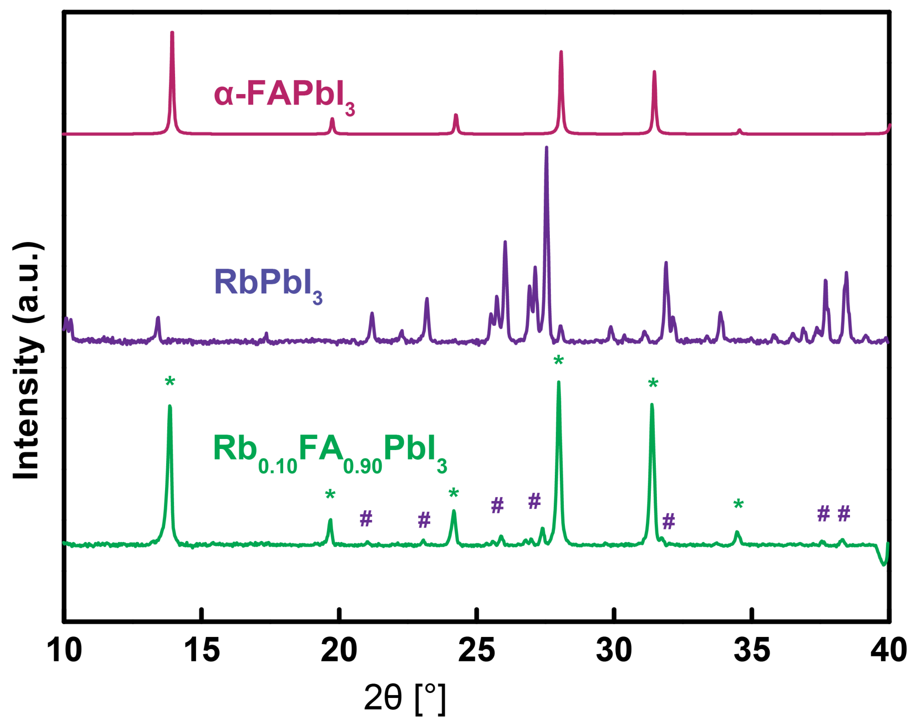

Figure S4. pXRD pattern for the $RbPbI_3$ and $Rb_{0.10}FA_{0.90}$ compositions. Asterisks (*) indicate the primary phase, hashes (#) indicate the phase separated $RbPbI_3$.

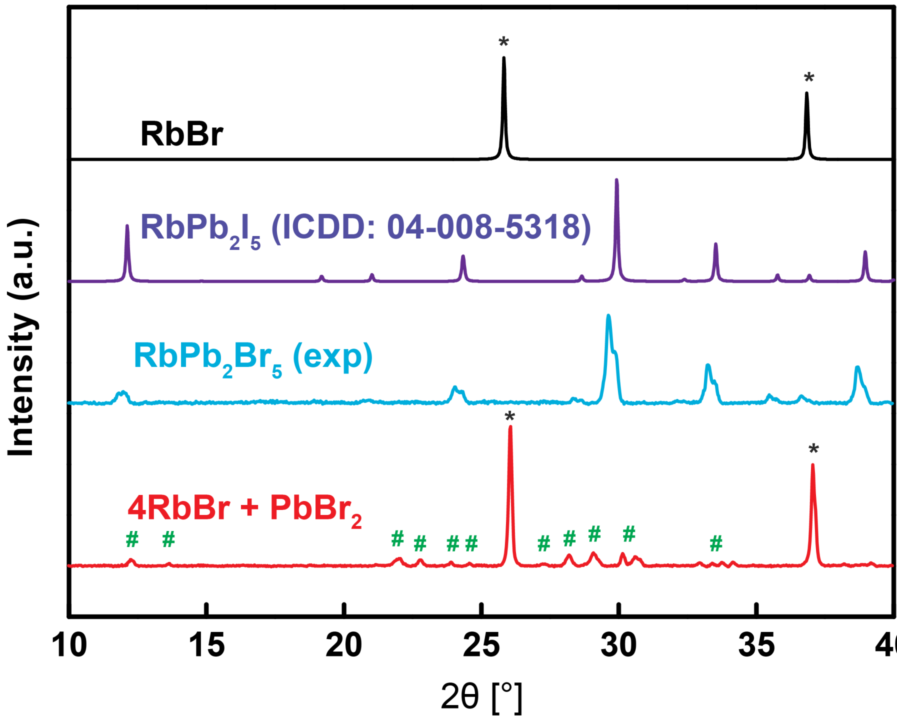

Figure S5. pXRD pattern for the rubidium lead bromides. Asterisks (*) indicate RbBr, hashes (#) indicate "phase X".

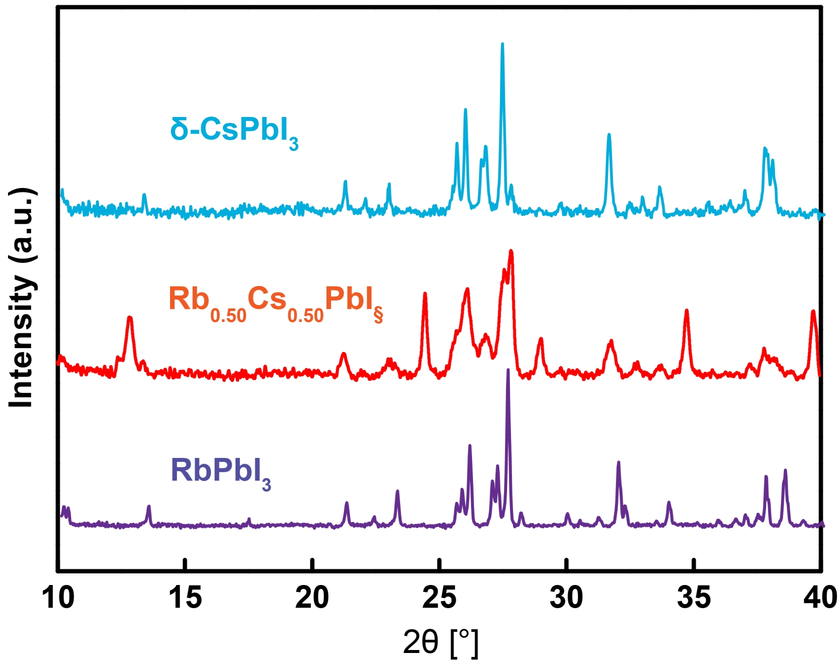

Figure S6. pXRD data for $Cs_{0.50}Rb_{0.50}PbI_3$.

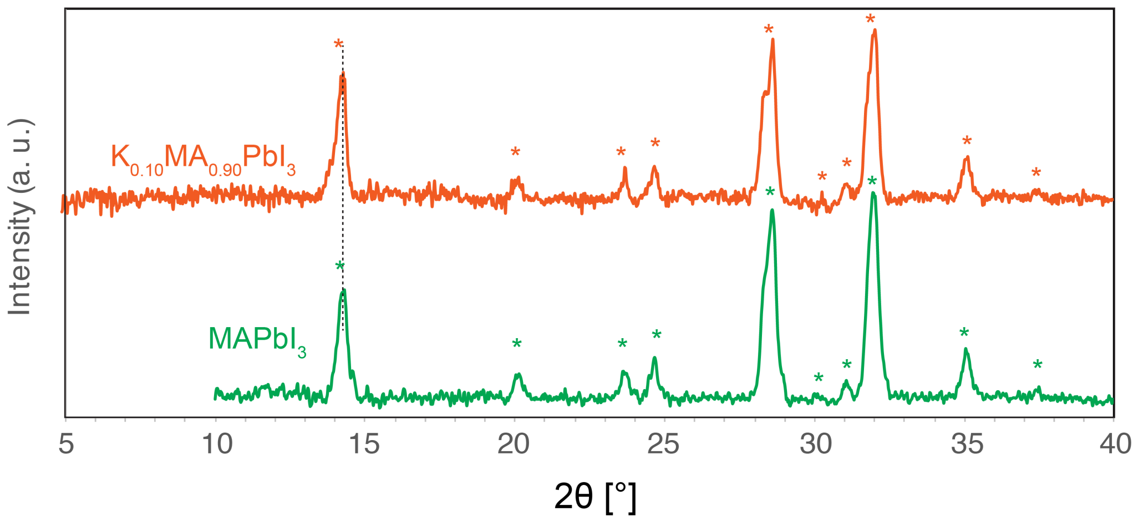

Figure S7. pXRD data for $K_{0.10}MA_{0.90}PbI_3$. Asterisks (*) indicate the primary $MAPbI_3$ phase.

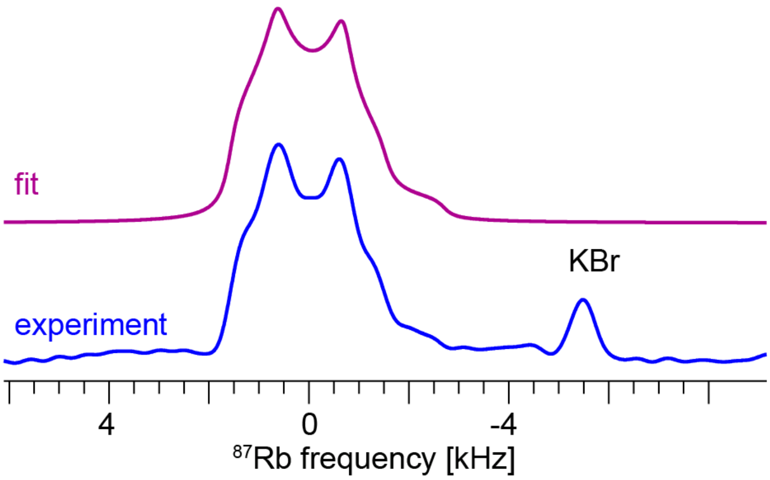

Figure S8. Experimental and fitted ^{87}Rb MAS (20 kHz) spectrum of the compound obtained by grinding 4 eq. RbI with 1 eq. PbI_2 (refered to as "phase X" in the manuscript).

C_Q=3.41 MHz
η=0.373
δ_{iso}=72.3 ppm (rel. to RbI)

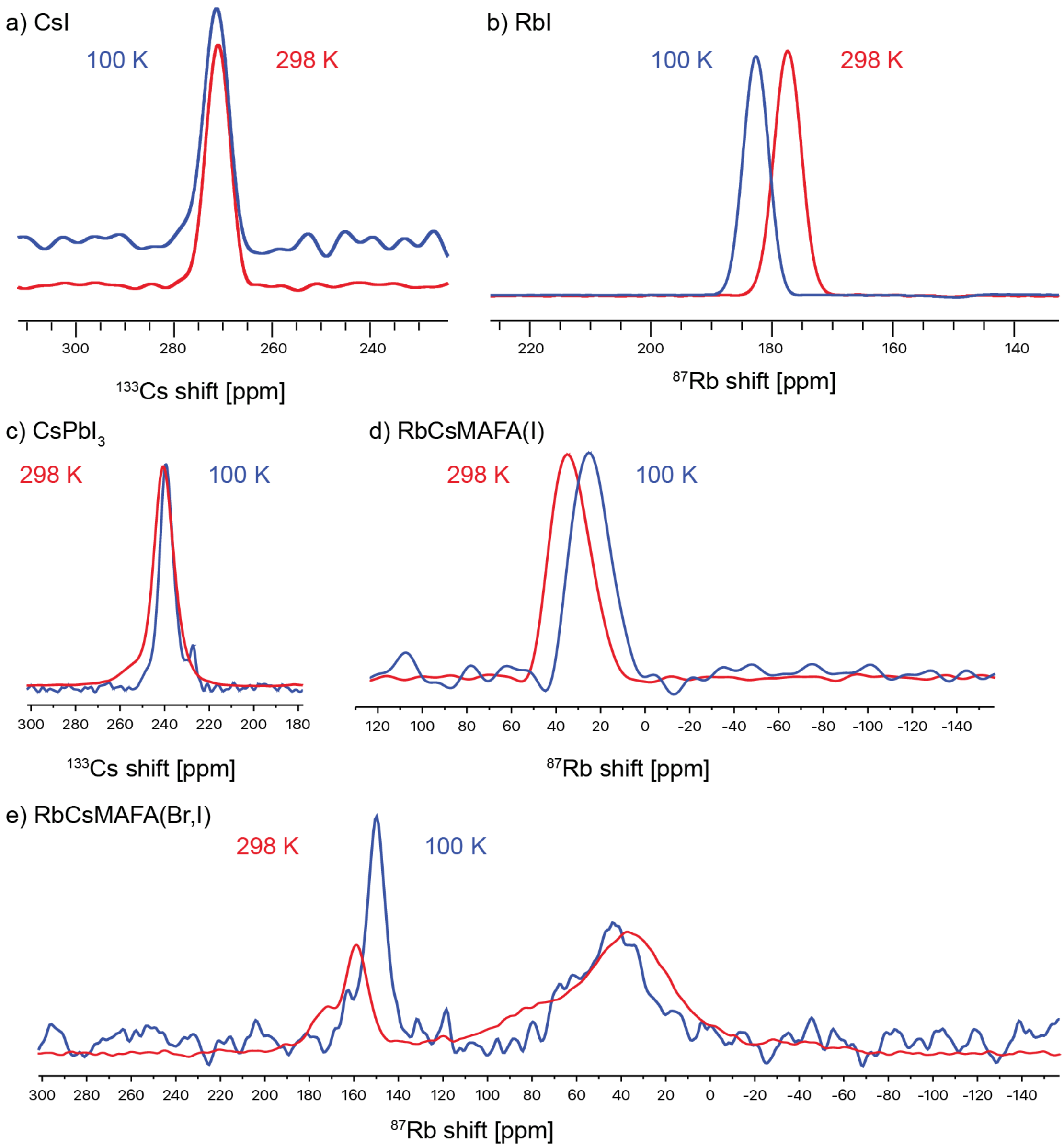

Figure S9. A comparison between 298 K and 100 K MAS spectra of (a) CsI, (b) RbI, (c) δ-$CsPbI_3$, (d) RbCsMAFA(I), (e) RbCsMAFA(Br,I).

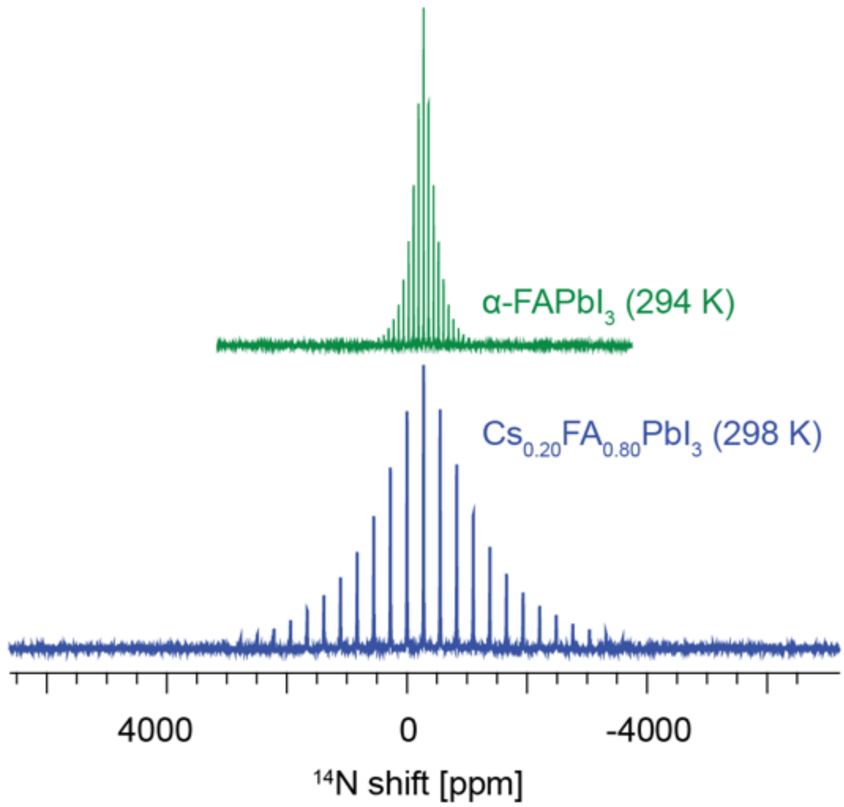

Figure S10. ^{14}N MAS spectra of α-$FAPbI_3$ and $Cs_{0.20}FA$.

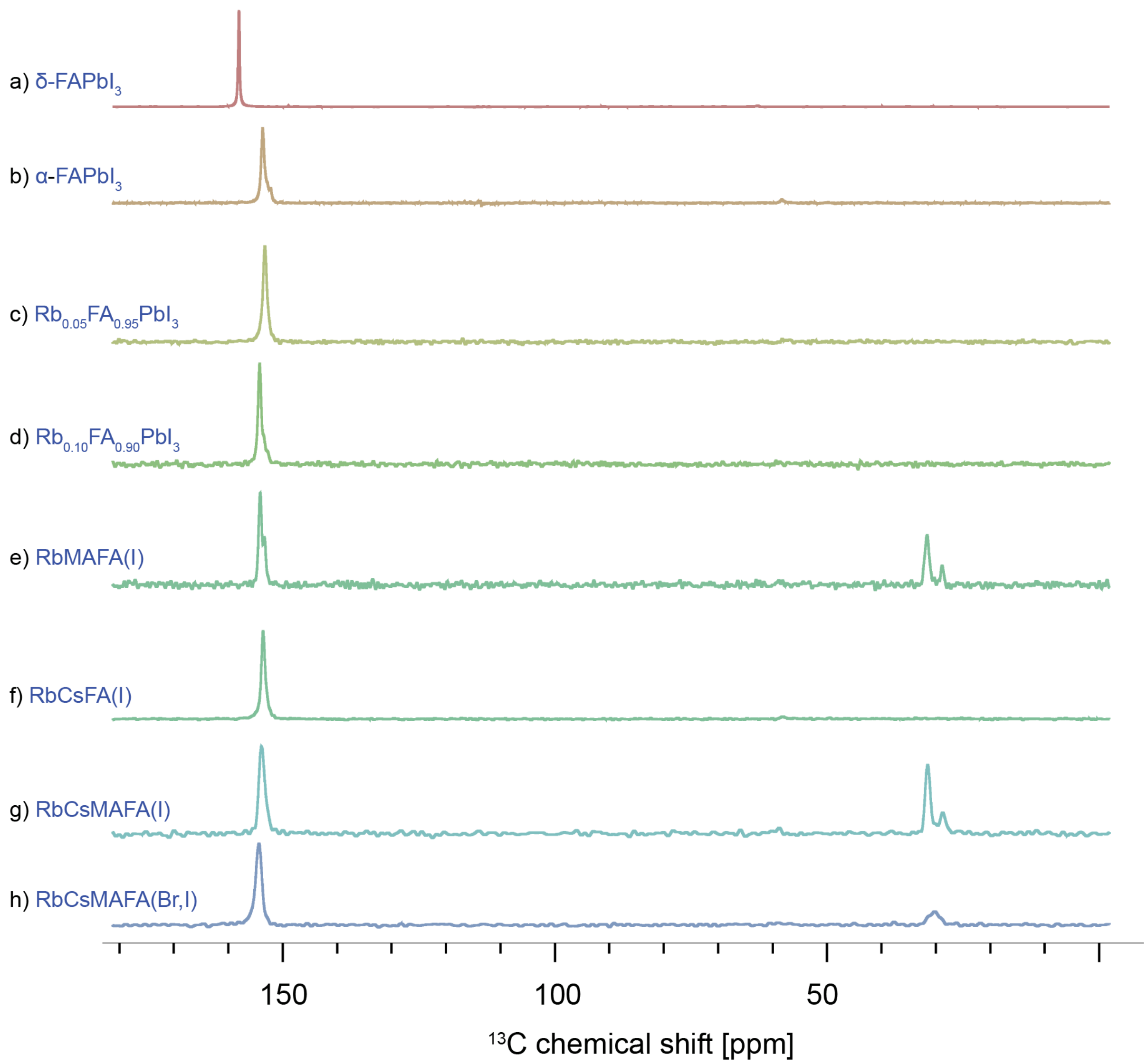

Figure S11. Low-temperature (100 K) ^{13}C CP MAS spectra of the materials studied in this work.

Details of DFT calculations of ^{133}Cs and ^{87}Rb shifts

Cluster generation

The crystal structures of CsI,[4] RbI,[5] cubic (black) and hexagonal (yellow) $FAPbI_3$[6], tetragonal (black) $MAPbI_3$[7] , hexagonal (yellow) $CsPbI_3$[8] and hexagonal (yellow) $RbPbI_3$[8] were used as a starting point for the clusters. The remaining crystal structures (cubic $RbPbI_3$, cubic $CsPbI_3$ and tetragonal $CsPbI_3$) were generated by replacing the FA/MA cations corresponding cubic/tetragonal crystal structure by Cs/Rb cations.

Next, the proton positions in the periodic black $FAPbI_3$ structure as well as the Cs/Rb positions in the substituted periodic structures were optimized using density functional theory (DFT) at the generalized gradient approximation (GGA) level with the PBE[9] functional including relativistic effects (with spin-orbit coupling) and the Grimme[10] dispersion correction within the Quantum Espresso suite[11]. In every calculation a plane-wave maximum cutoff energy of 90 Ry and a 3x3x3 Monkhorst-Pack[12] grid of k-points was employed.

The final clusters were generated as a central cation surrounded by a PbI_3 cage representing the asymmetric unit of the periodic crystal structure. To ensure charge compensation and cluster symmetry additional cations surrounding the PbI_3 cage were included. Generic models of the generated clusters are depicted in fig. S12.

The mixed FA/(Rb/Cs) clusters were assembled from the relaxed black $FAPbI_3$ structure by replacing the central FA^+ cation with a Cs^+/Rb^+ cation.

The procedure described above leads to the cluster $Cs_{32}I_{32}$, $Rb_{14}I_{14}$, cubic and tetragonal $Cs_{20}Pb_8I_{36}$, cubic $XFA_{19}Pb_8I_{36}$ and hexagonal $X_{18}Pb_6I_{30}$ (with X = Rb/Cs). For the hexagonal $RbPbI_3$ structure the chemical shifts were also calculated with a larger cluster ($Rb_{20}Pb_8I_{36}$). They were within 1 ppm agreement of the shifts calculated for the smaller cluster ($Rb_{18}Pb_6I_{30}$).

In general, the setup of the clusters, with respect to level of theory, charge compensation and cluster symmetry, was done according to recent studies on calculations of electronic and magnetic properties of heavy atoms.[13-18]

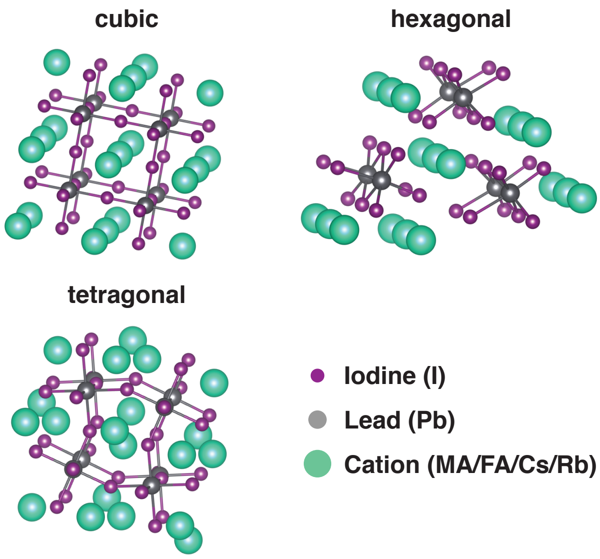

Figure S12. Example clusters used in DFT chemical shift calculations.

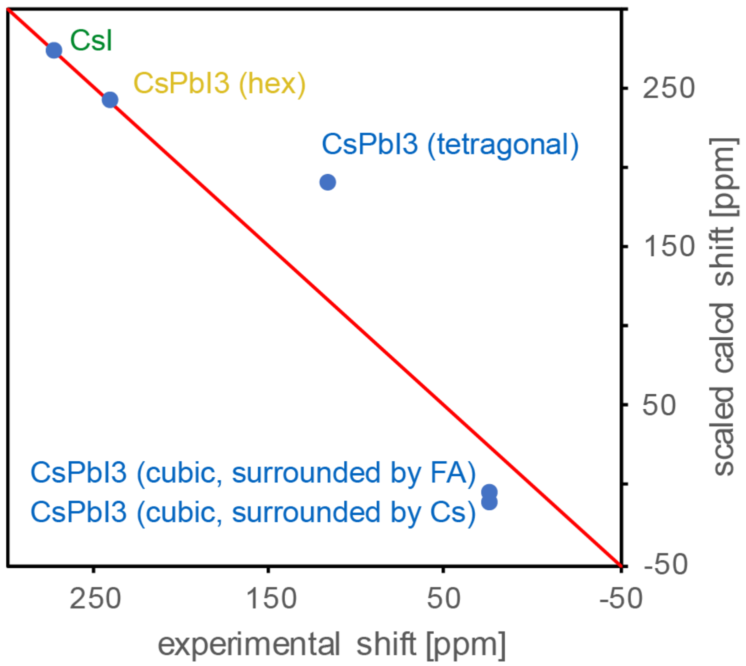

Figure S13. A correlation between the experimental and scaled calculated ^{133}Cs shift for a series of structures (with CsI and δ-$CsPbI_3$ used as references).

References

1. Prochowicz, D.; Yadav, P.; Saliba, M.; Saski, S. M.; Zakeeruddin, S. M.; Lewinski, J.; Gratzel, M., *Sustainable Energy and Fuels* **2017,** *1*, 689-693.
2. Saliba, M.; Matsui, T.; Seo, J. Y.; Domanski, K.; Correa-Baena, J. P.; Nazeeruddin, M. K.; Zakeeruddin, S. M.; Tress, W.; Abate, A.; Hagfeldt, A.; Gratzel, M., *Energy & Environmental Science* **2016,** *9* (6), 1989-1997.
3. Saliba, M.; Matsui, T.; Domanski, K.; Seo, J. Y.; Ummadisingu, A.; Zakeeruddin, S. M.; Correa-Baena, J. P.; Tress, W. R.; Abate, A.; Hagfeldt, A.; Gratzel, M., *Science* **2016,** *354* (6309), 206-209.
4. Huang, T. L.; Ruoff, A. L., *Physical Review B* **1984,** *29* (2), 1112-1114.
5. van den Bosch, A.; Vansummeren, J.; Dresselaers, J.; Hovi, M., *Physica Status Solidi a-Applications and Materials Science* **1972,** *11* (2), 479-482.
6. Weller, M. T.; Weber, O. J.; Frost, J. M.; Walsh, A., *Journal of Physical Chemistry Letters* **2015,** *6* (16), 3209-3212.
7. Weber, D., *Zeitschrift Fur Naturforschung Section B-a Journal of Chemical Sciences* **1978,** *33* (12), 1443-1445.
8. Trots, D. M.; Myagkota, S. V., *Journal of Physics and Chemistry of Solids* **2008,** *69* (10), 2520-2526.
9. Perdew, J. P.; Burke, K.; Ernzerhof, M., *Physical Review Letters* **1997,** *78* (7), 1396-1396.
10. Grimme, S., *Journal of Computational Chemistry* **2006,** *27* (15), 1787-1799.
11. Giannozzi, P.; Baroni, S.; Bonini, N.; Calandra, M.; Car, R.; Cavazzoni, C.; Ceresoli, D.; Chiarotti, G. L.; Cococcioni, M.; Dabo, I.; Dal Corso, A.; de Gironcoli, S.; Fabris, S.; Fratesi, G.; Gebauer, R.; Gerstmann, U.; Gougoussis, C.; Kokalj, A.; Lazzeri, M.; Martin-Samos, L.; Marzari, N.; Mauri, F.; Mazzarello, R.; Paolini, S.; Pasquarello, A.; Paulatto, L.; Sbraccia, C.; Scandolo, S.; Sclauzero, G.; Seitsonen, A. P.; Smogunov, A.; Umari, P.; Wentzcovitch, R. M., *Journal of Physics-Condensed Matter* **2009,** *21* (39).
12. Pack, J. D.; Monkhorst, H. J., *Physical Review B* **1977,** *16* (4), 1748-1749.
13. Giorgi, G.; Yoshihara, T.; Yamashita, K., *Physical Chemistry Chemical Physics* **2016,** *18* (39), 27124-27132.
14. Alkan, F.; Dybowski, C., *Journal of Physical Chemistry A* **2016,** *120* (1), 161-168.
15. Dmitrenko, O.; Bai, S.; Beckmann, P. A.; van Bramer, S.; Vega, A. J.; Dybowski, C., *Journal of Physical Chemistry A* **2008,** *112* (14), 3046-3052.
16. Even, J.; Pedesseau, L.; Jancu, J. M.; Katan, C., *Journal of Physical Chemistry Letters* **2013,** *4* (17), 2999-3005.
17. Alkan, F.; Dybowski, C., *Physical Chemistry Chemical Physics* **2014,** *16* (27), 14298-14308.
18. Alkan, F.; Dybowski, C., *Physical Chemistry Chemical Physics* **2015,** *17* (38), 25014-25026.